Optimized calibration strategy for high order adaptive optics systems in closed-loop: the slope-oriented Hadamard actuation

Serge Meimon, Cyril Petit, Thierry Fusco

Optimized calibration strategy for high order adaptive optics systems in closed-loop: the slope-oriented Hadamard actuation

Serge Meimon,* Cyril Petit, and Thierry Fusco

Onera - The French Aerospace Lab
F-92322 Châtillon, France
**serge.meimon@onera.fr*

Abstract: The accurate calibration of the interaction matrix affects the performance of an adaptive optics system. In the case of high-order systems, when the number of mirror modes is worth a few thousands, the calibration strategy is critical to reach the maximum interaction matrix quality in the minimum time. This is all the more true for the future European Extremely Large Telescope. Here, we propose a novel calibration scheme, the Slope-Oriented Hadamard strategy. We then build a tractable interaction matrix quality criterion, and show that our method tends to optimize it. We demonstrate that for a given level of quality, the calibration time needed using the Slope-Oriented Hadamard method is seven times less than with a classical Hadamard scheme. These analytic and simulation results are confirmed experimentally on the SPHERE XAO system (SAXO).

OCIS codes: (010.1080) Active or adaptive optics; (010.1330) Atmospheric turbulence; (110.6770) Telescopes.

References and links

1. Y. Clenet, M. E. Kasper, N. Ageorges, C. Lidman, T. Fusco, O. Marco, M. Hartung, D. Mouillet, B. Koehler, G. Rousset, and N. N. Hubin, "Naco performance: status after 2 years of operation," Proc. SPIE **5490**, 107–117 (2004).
2. T. Fusco, J.-F. Sauvage, C. Petit, A. Costille, K. Dohlen, D. Mouillet, J.-L. Beuzit, M. Kasper, M. Suarez, C. Soenke, E. Fedrigo, M. Downing, P. Baudoz, A. Sevin, D. Perret, A. Barrufolo, B. Salasnich, P. Puget, F. Feautrier, S. Rochat, T. Moulin, A. Deboulb, E. Hugot, A. Vigan, D. Mawet, J. Girard, and N. Hubin, "Final performance and lesson-learned of saxo, the vlt-sphere extreme ao: from early design to on-sky results," Proc. SPIE **9148**, 91481U (2014).
3. C. Petit, J.-F. Sauvage, A. Sevin, A. Costille, T. Fusco, P. Baudoz, J.-L. Beuzit, T. Buey, J. Charton, K. Dohlen, P. Feautrier, E. Fedrigo, J.-L. Gach, N. Hubin, E. Hugot, M. Kasper, D. Mouillet, D. Perret, P. Puget, J.-C. Sinquin, C. Soenke, M. Suarez, and F. Wildi, "The sphere XAO system SAXO: integration, test, and laboratory performance," Proc. SPIE **8447**, 84471Z (2012).
4. A. Riccardi, G. Brusa, P. Salinari, D. Gallieni, R. Biasi, M. Andrighettoni, and H. M. Martin, "Adaptive secondary mirrors for the large binocular telescope," Proc. SPIE **4839**, 721–732 (2003).
5. S. Oberti, F. Quiros-Pacheco, S. Esposito, R. Muradore, R. Arsenault, E. Fedrigo, M. Kasper, J. Kolb, E. Marchetti, A. Riccardi, C. Soenke, and S. Stroebele, "Large DM AO systems: synthetic IM or calibration on sky?" Proc. SPIE **6272**, 627220 (2006).
6. C. Béchet, J. Kolb, P.-Y. Madec, M. Tallon, and E. Thibaut, "Identification of system misregistrations during ao-corrected observations" in *Second International Conference on Adaptive Optics for Extremely Large Telescopes*, (2011), p. 61.
7. C. Boyer, V. Michau, and G. Rousset, "Adaptive optics: interaction matrix measurements and real time control algorithms for the come-on project," Proc. SPIE **1271**, 63–81 (1990).

#245856 Received 13 Jul 2015; revised 2 Sep 2015; accepted 2 Sep 2015; published 7 Oct 2015

8. Y. Guo, C. Rao, H. Bao, A. Zhang, X. Zhang, and K. Wei, "Multichannel-hadamard calibration of high-order adaptive optics systems," Opt. Express **22**, 13792–13803 (2014).
9. M. Kasper, E. Fedrigo, D. P. Looze, H. Bonnet, L. Ivanescu, and S. Oberti, "Fast calibration of high-order adaptive optics systems," J. Opt. Soc. Am. A **21**, 1004–1008 (2004).

1. Introduction

Ground based telescopes image quality is limited by fast evolving phase distortions induced by the atmospheric turbulence. Adaptive optics (AO) systems aim at compensating in real time these wave-front distortions by actuating a wave-front correction device such as a deformable mirror. To do so, a wave-front sensor (WFS) measures the residual aberrations downstream the deformable mirror (DM), and and a real time computer converts these measurements into commands to be sent to the correction device. This process, looped at a high frame rate (typically several hundred Hertz), relies on a linear model of the interaction between the N_{act} deformable mirror commands $u = \{u_1, \ldots, u_{N_{\text{act}}}\}$ and the N_{slope} WFS measurements $y = \left\{y_1, \ldots, y_{N_{\text{slope}}}\right\}$, *e.g.* the slope measurements in the classical case of Shack-Hartmann WFS. This linear model, embodied by the $N_{\text{slope}} \times N_{\text{act}}$ interaction matrix D stacking the WFS response to each DM mode, is generally identified prior to observation using an internal calibration source.

This calibration process is getting more and more complex due recent evolution of AO for astronomy: the dramatic degree of freedom increase - from 185 actuators and 288 WFS measurements for NACO [1] in 2001 to 1377 actuators and 2480 WFS measurements for SAXO [2, 3] in 2013 - demands a fast calibration strategy; the advent of active/adaptive primary or secondary mirrors [4], for which an internal calibration source is not available, has led to considering on-sky calibration schemes. The high number of degrees of freedom reduces the calibration time per mode. Even with powerful calibration sources, new calibration strategies are required to improve the signal to noise ratio. This is all the more true for on-sky measurements where turbulence acts as supplementary zero-mean measurement noise.

For this reason, some teams resolve to using synthetic interaction matrices [5]. An original strategy proposed by Bechet *et al.* [6] consists in refining the estimation of the interaction matrix during closed loop operation, but the performance of such a method is difficult to assess in the general case as they are dependent on the system used and on the turbulence statistics. Moreover, specific on-sky calibration issues are outside the scope of this paper.

Successful results have been obtained by optimizing the actuation patterns used during the calibration. The standard push-pull "Zonal" method [7] consists in calibrating one actuator at a time, and measuring the WFS response difference between a push and a pull (this procedure enables to cancel out static aberrations). The essential flaw of this method is that the signal is concentrated on one local actuator region on the pupil, while the measurements corresponding to the rest of the pupil convey only noise. New calibration strategies have then been proposed which involve several actuators at a time : multichannel actuation [8], which proposes to calibrate sets of actuators far enough from each other, so that their associated WFS responses can be considered spatially independent and thus disentangled; Hadamard actuation [9], which generalizes this approach by considering mathematically independent actuation patterns made of Hadamard vectors, carrying more "energy" than pushing or pulling a single actuator. These patterns correspond to maximal energy actuation patterns under a maximum voltage constraint $u < u_{\text{max}}$, dictated by the working domain of the DM. The patterns obtained with this method contain only $\pm u_{\text{max}}$ values.

Although this Hadamard "voltage oriented" actuation method has led to major progress in interaction matrix calibration quality, it is not fully adapted to for closed-loop systems. For instance, the u_{max} value is never set in practice to the maximum voltage admissible by the DM. Indeed, in closed-loop the WFS has a much smaller linearity range (suited to measure the

#245856 Received 13 Jul 2015; revised 2 Sep 2015; accepted 2 Sep 2015; published 7 Oct 2015

residual turbulence) than the deformable mirror (suited to correct for the *total* turbulence). In the calibration process, the actuation pattern amplitudes are rather dictated by the wave-front linearity range. More generally, the choice of a set of calibration patterns has to be thought in the measurement space. Let us consider here the case of a Shack-Hartmann wave-front sensor, for which the WFS measurements are slope measurements (although these developments may largely be extended to other WFS technologies). The goal here is then to maximize the energy of the slope signal to overcome the impact of slope measurement noise (due to detector noise or turbulence), under a maximum slope constraint (considering the saturation of the Shack-Hartmann wave-front sensor slopes).

We therefore propose in this paper a "slope-oriented" Hadamard actuation scheme. After recalling the principles of standard "Zonal" and "voltage-oriented" Hadamard methods, we first describe how we achieve such a "slope-oriented" scheme (section 2). Then we compute an interaction matrix calibration error metric, which we use to compare the "Zonal", "voltage-oriented" Hadamard and "slope-oriented" Hadamard strategies in the configuration of SPHERE's extreme AO system SAXO [2, 3] (section 3). The results obtained are then confirmed on an end-to-end simulation of SAXO (section 4). Last we report experimental results (section 5) obtained on SAXO during Assembly, Integration and Test (AIT) .

2. Standard "zonal," "voltage-oriented Hadamard" and "slope oriented Hadamard" schemes

Let M_{DM} be the influence function matrix, giving the modal decomposition of the phase shape of the mirror for a unitary displacement of each actuator. We suppose, with no lack of generality, that the phase modal basis size is very high, so the under-representation issues remain negligible. Let M_{WFS} be the matrix containing the WFS measurements for each phase mode. The interaction matrix D gives the WFS measurements for a unitary displacement of each actuator:

$$D = M_{\mathrm{WFS}} \cdot M_{\mathrm{DM}}. \tag{1}$$

The calibration procedure of the interaction matrix consists in sending a set of N_{cal} actuation patterns $\{u_1, \ldots, u_{N_{\mathrm{cal}}}\}$ and to measure the corresponding WFS measurements $\{y_1, \ldots, y_{N_{\mathrm{cal}}}\}$. The measurement y_n corresponding to pattern u_n is affected by a measurement noise w_n, and by the presence of a turbulent phase φ_n during the calibration:

$$y_n = Du_n + w_n + M_{\mathrm{WFS}}\varphi_n \tag{2}$$

with D the interaction matrix to identify. Denoting U, Y, W, ϕ the matrices which rows are the u_n, y_n, w_n, φ_n, we obtain:

$$Y = DU + W + M_{\mathrm{WFS}}\phi \tag{3}$$

The estimated interaction matrix is retrieved by multiplying the measurement matrix Y by the pseudo-inverse $U^\dagger$ of U:

$$\hat{D} = Y \cdot U^\dagger = DU \cdot U^\dagger + W \cdot U^\dagger + M_{\mathrm{WFS}}\phi \cdot U^\dagger. \tag{4}$$

Provided that U is full rank, *i.e.* that the calibration pattern set used is rich enough to span all the shapes achievable by the DM, we have $U \cdot U^\dagger = \mathbf{I}\mathrm{d}$, $\mathbf{I}\mathrm{d}$ denoting the identity matrix (in this case with a dimension N_{act}). The calibration error is then given by

$$\Delta D \triangleq D - \hat{D} = -\underbrace{\left(M_{\mathrm{WFS}} \cdot \phi + W\right)}_{\bar{W}} \cdot U^\dagger \tag{5}$$

#245856 Received 13 Jul 2015; revised 2 Sep 2015; accepted 2 Sep 2015; published 7 Oct 2015

To minimize this error, one may minimize the perturbation $\bar{W} = M_{\mathrm{WFS}} \cdot \phi + W$ by using when possible an internal calibration source: the turbulence ϕ then reduces to the local turbulence in the bench, and with a bright source, the noise term W can be kept low enough.

The dimension of the interaction matrix is $N_{\mathrm{slope}} \times N_{\mathrm{act}}$, with N_{act} being the number of actuators of the deformable mirror, and N_{slope} the number of measurements provided by the WFS at each frame (for a Shack-Hartmann WFS, it corresponds to twice the number of valid sub-apertures). This means that N_{act} independent patterns at least have to be applied. When for some systems N_{act} reaches several thousands, this procedure can become very time consuming. The goal is then to make an optimal use of the incoming photons, by generating the most "energetic" WFS response possible.

The standard Zonal method [7] consists in pushing one actuator at a time with a voltage u, which corresponds to a diagonal matrix U:

$$U = u \cdot \mathbf{I}\mathrm{d} \Rightarrow \Delta D = -\bar{W}/u \tag{6}$$

u has then to be set at the maximum value compatible with the system, *i.e.* without saturating the WFS nor the deformable mirror.

If one considers only the deformable mirror *voltage* saturation $u < u_{\max}$, the optimal solution (with respect to a quadratic norm on ΔD) is

$$U = u_{\max} \cdot H \tag{7}$$

with H a Hadamard matrix, which contains only -1 and 1 values [9]. However, this Hadamard "voltage oriented" actuation scheme is not suited to closed-loop systems for which the WFS has a much smaller linearity range (suited to measure the *residual* turbulence) than the deformable mirror (suited to correct for the *total* turbulence). We propose here a Hadamard "slope oriented" actuation scheme obtained by considering the saturation of the Shack-Hartmann WFS slopes.

We consider here only the WFS measurement saturation $s < s_{\max}$. The most effective calibration patterns are the one that take all the spots at the limits of the linear range of the WFS, *i.e.* at slopes $s = \pm s_{\max}$. The problem here is then to find a set of actuation patterns U such that DU contains $\pm s_{\max}$ values. U shall also have a rank superior or equal to the number of actuators, so that the whole deformable mirror shape space is spanned (this ensures $UU^{\dagger} = \mathbf{I}\mathrm{d}$). The way we find such a U consists in three steps:

1. obtain a first rough estimate of D_0 (a synthetic matrix can be used);
2. solve for $DU = s_{\max}H$, with H a Hadamard matrix ($s_{\max}H$ contains only $\pm s_{\max}$ values). This is done using D_0 :$U_0 = D_0^{\dagger} \cdot s_{\max}H$;
3. perform a linear iterative minimization of $\sum_{i,j} \left| \left| [D_0 U]_{i,j} \right|^2 - s_{\max}^2 \right|^2$ with respect to U, starting from U_0.

The set of actuation patterns U obtained with this iterative is probably not optimal. There may exist an algorithm able to identify U with a rank superior or equal to the number of actuators, yielding the lowest interaction matrix calibration error while saturating neither the deformable mirror nor the WFS. However, the process described here provides a decent approximation of this optimal solution.

We have used this strategy on the SPHERE's extreme AO system SAXO case [2, 3] (1377 actuator CILAS SAM deformable mirror with 25% coupling, 1240 sub-aperture Shack-Hartmann WFS with 6×6 pixels per sub-aperture). The theoretical histograms of the slopes DU obtained during the interaction matrix calibration for the zonal, voltage-oriented and slope oriented Hadamard strategies are shown in Fig. 1.

#245856 Received 13 Jul 2015; revised 2 Sep 2015; accepted 2 Sep 2015; published 7 Oct 2015

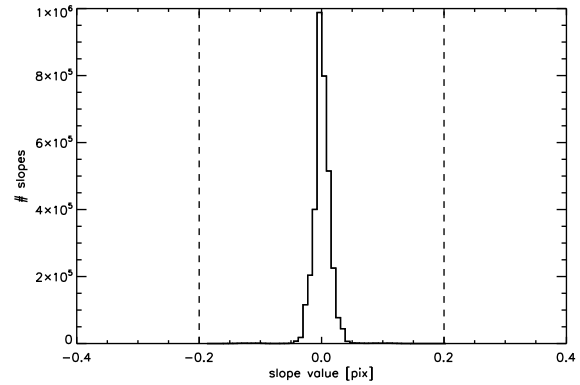

(a) Zonal

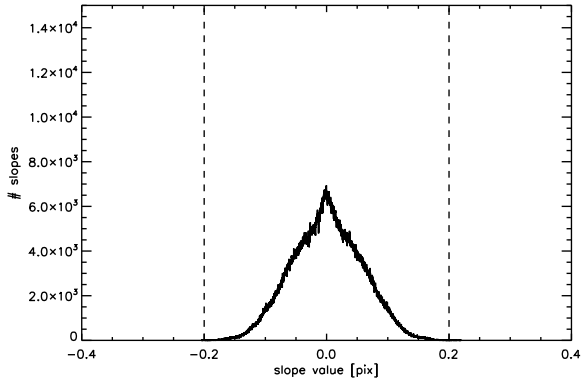

(b) Voltage-oriented Hadamard

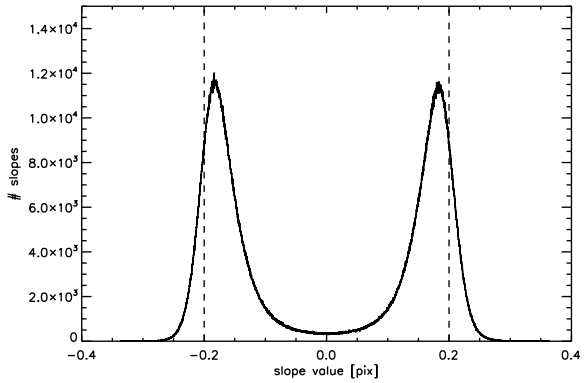

(c) Slope-oriented Hadamard

Fig. 1. Theoretical histograms of the slopes *DU* obtained during the interaction matrix calibration for the standard "Zonal" (a), "voltage-oriented" Hadamard (b) and "slope-oriented" Hadamard (c) strategies. Dashed lines correspond to $\pm s_{\max}$.

#245856 Received 13 Jul 2015; revised 2 Sep 2015; accepted 2 Sep 2015; published 7 Oct 2015

We see that the slope-oriented strategy yields the most energetic slope patterns. Intuitively, the most efficient calibration method is the one yielding the highest signal to noise ratio, *i.e.* yielding the most energetic WFS signal for a given level of calibration noise. The calibration error propagated in the AO closed loop should therefore be lower. Indeed, the way we eventually assess the quality of an interaction matrix is the performance of a loop closed with this interaction matrix. The question is : how does this compares with the noise level on the interaction matrix, as witnessed when the matrix is graphically displayed? In the next section, we express the part of the residual phase variance due to interaction matrix miscalibration, in a simplified adaptive optics loop configuration. We discuss the difference between this metric and a more intuitive one $\left\|D-\hat{D}\right\|^2$.We then use this metric to compare the standard "Zonal," "voltage-oriented" Hadamard and "slope-oriented" Hadamard strategies.

3. A metric for assessing the interaction matrix quality

Let y_n the WFS measurements at frame n and w_n the corresponding noise. Let u_n be the DM actuator voltages at frame n, and φ_n (or φ_n^{res}) the turbulent (or residual) phase at frame n. We describe the AO system with the following model, corresponding to a simplified 1 frame delay loop:

$$\begin{cases} y_n = M_{\text{WFS}} \cdot \varphi_{n-1}^{\text{res}} + w_n \\ \varphi_n^{\text{res}} = \varphi_n - M_{\text{DM}} \cdot u_n \\ u_n = u_{n-1} + gM_{\text{cont}} y_n \end{cases} \tag{8}$$

By expressing $\varphi_n^{\text{res}} - \varphi_{n-1}^{\text{res}}$ with the second line of Eq. (8), we derive:

$$\varphi_n^{\text{res}} = \underbrace{\varphi_n - \varphi_{n-1}}_{temporal} + \underbrace{(\mathbf{Id} - M_{\text{DM}} \cdot gM_{\text{cont}} \cdot M_{\text{WFS}}) \cdot \varphi_{n-1}^{\text{res}}}_{system} - \underbrace{M_{\text{DM}} \cdot gM_{\text{cont}} \cdot w_n}_{WFSnoise} \tag{9}$$

In this expression, g is a gain set to value different from 1 for stability reasons, and M_{cont} can be chosen different from $D^\dagger$ in some control strategies (for example requiring the filtering of some specific mode).

The following derivation is only heuristic, and aims only at isolating a tractable expression of the miscalibration error. The system part can be divided as:

$$\begin{aligned} \varphi_n^{\text{res},system} &= (\mathbf{Id} - M_{\text{DM}} \cdot gM_{\text{cont}} \cdot M_{\text{WFS}}) \cdot \varphi_{n-1}^{\text{res}} \\ &= \underbrace{\left(\mathbf{Id} - M_{\text{DM}} \cdot D^\dagger \cdot M_{\text{WFS}}\right) \cdot \varphi_{n-1}^{\text{res}}}_{fitting,aliasing} \\ &\quad + \underbrace{M_{\text{DM}} \cdot \left(D^\dagger - \hat{D}^\dagger\right) \cdot M_{\text{WFS}} \cdot \varphi_{n-1}^{\text{res}}}_{\varphi_n^{\text{res},miscal} = \text{miscalibration error}} \\ &\quad + \underbrace{M_{\text{DM}} \cdot \left(\hat{D}^\dagger - gM_{\text{cont}}\right) \cdot M_{\text{WFS}} \cdot \varphi_{n-1}^{\text{res}}}_{\text{stability margin, control strategy}} \end{aligned} \tag{10}$$

The miscalibration term $\varphi_n^{\text{res},miscal}$ contains the difference $D^\dagger - \hat{D}^\dagger$, which we would like to link to $\Delta D \triangleq D - \hat{D}$ of Eq. (5). To do so, we need to make the assumption that the deformable mirror unseen modes have been filtered out, or conversely that M_{DM} contains no mode unseen by the WFS. With this assumption, we derive the following expression of the miscalibration

#245856 Received 13 Jul 2015; revised 2 Sep 2015; accepted 2 Sep 2015; published 7 Oct 2015

error phase variance (see appendix A):

$$\mathscr{E}(\Delta D) = \text{Var}\ \varphi_n^{\text{res},miscal} \simeq \left\| M_{\text{WFS}}^{\dagger} \cdot \Delta D \cdot D^{\dagger} \right\|^2_{\mathscr{C}_{\text{slope}}}, \tag{11}$$

with $\|X\|^2_{\mathscr{C}_{\text{slope}}} = X^{\text{T}} \mathscr{C}_{\text{slope}} X$ and $\mathscr{C}_{\text{slope}}$ the covariance matrix of the residual slopes $M_{\text{WFS}} \cdot \varphi_{n-1}^{\text{res}}$. Once again, this expression was obtained heuristically (for instance, the three terms in Eq. (10) are not statistically independent), and is by no means a rigorous derivation of the miscalibration contribution to the error budget. But it helps showing that the interaction matrix calibration error ΔD impacts the overall performance depending on the statistics of the residual slopes presented to the WFS (embodied by $\mathscr{C}_{\text{slope}}$). The term $M_{\text{WFS}}^{\dagger}$ converts slopes (in arbitrary units such as centroid displacements in pixels) in wave-front error in radians, with a physical meaning.

Therefore, we use the metric $\mathscr{E}$ to select the best actuation pattern U for the calibration. To do so, we insert Eq. (5) in the expression of $\mathscr{E}$ of Eq. (11). With simplifying assumptions on the calibration noise and slopes statistics, we derive the following expression (see appendix B)

$$\mathscr{E}(\Delta D) \propto \left\| (DU)^{\dagger} \right\|^2 \tag{12}$$

The best actuation strategy would then be to minimize the squared norm of $(DU)^{\dagger}$. The intuitive strategy we followed to produce the slope-oriented Hadamard Actuation method led to maximizing the squared norm of DU, *i.e.* to obtain the highest slopes values during the calibration (while keeping them within the WFS linearity range) as emphasized in Fig. 1 histograms. Indeed, the values of $\mathscr{E}(\Delta D)$ obtained with the simplified expression of Eq. (12) for the zonal, voltage-oriented and slope-oriented Hadamard strategies (corresponding to the DU values shown in Fig. 1) are presented in Table 1.

Table 1. Comparison of the miscalibration error metric values obtained for the zonal, voltage-oriented and slope-oriented Hadamard strategies in the SAXO configuration (computed from the DU values shown in Fig. 1).

	Zonal	voltage-oriented	slope-oriented
$\propto \mathscr{E}(\Delta D)$	1	0.012	0.0017
$\propto \mathscr{E}^{-1}(\Delta D)$	1	81	582

This shows that our slope-oriented strategy would yields a 582 gain over the zonal strategy, and nearly a factor 10 gain over the voltage-oriented Hadamard strategy, in terms of miscalibration error. In other words, the same quality could be obtained with the slope-oriented strategy in 12 seconds as with the voltage oriented strategy in 1.5 minutes or with the zonal strategy in 2 hours (assuming a photon noise regime during calibration).

We have therefore derived a heuristic interaction matrix quality metric corresponding to the contribution of the miscalibration error to the residual phase variance. With some simplifying assumptions, we have shown that minimizing this metric leads to choosing the actuation pattern that maximizes the slopes signal, which provides theoretical ground for our "slope-oriented" Hadamard calibration strategy.

4. Simulations

In order to confirm that our metric accurately conveys the induced error in closed loop, comprehensive simulations on an end-to-end simulator of SAXO [2, 3] have been conducted with the interaction matrices obtained for the three strategies, with various levels of noise on the Shack-Hartmann wave-front sensor during the interaction matrix calibration. The simulation

#245856 Received 13 Jul 2015; revised 2 Sep 2015; accepted 2 Sep 2015; published 7 Oct 2015

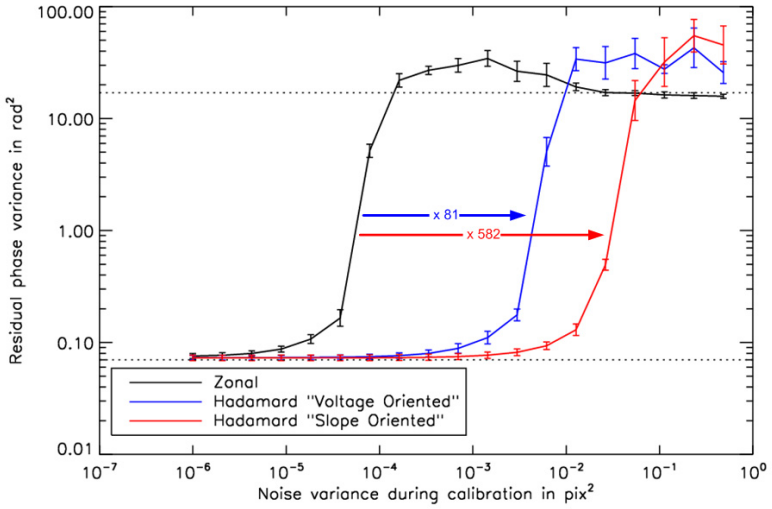

Fig. 2. End-to-end SAXO simulator results: residual phase variance obtained as a function of the WFS noise during the interaction matrix calibration. Simulation case: SAXO architecture (1377 SAM DM, 40x40 diffractive filtered Shack-Hartmann with weighted Center of Gravity), 1200Hz 2-frame delay loop, seeing = 0.85" [3].

case corresponded to a 0.85" seeing in the SAXO configuration [3]. Figure 2 plots the residual phase variance obtained as a function of the WFS noise during the interaction matrix calibration. The residual phase variance level in the low calibration noise regime corresponds to the other terms of the error budget (temporal error, aliasing and fitting errors, the noise error is negligible in this case as we simulated a high flux guide star). We see that the gaps between the curves follow exactly the values in Table 1. It confirms that our metric is suited to predict the closed loop residual phase error budget term due to interaction matrix miscalibration, and that the Slope Oriented Hadamard actuation should yield a factor 7 gain in calibration time compared to the Voltage Oriented method, and a factor 580 compared to the zonal method.

5. Experimental validation

To experimentally prove the applicability of the slope-oriented method, we have acquired three interaction matrices on the SAXO bench at Observatoire de Paris during AIT tests, with the three strategies, and considering a 90 seconds calibration time for each matrix. It corresponds to a flux worth 10 photons per subaperture and per frame (wave-front sensing is performed with EMCCD amplification leading to virtually 0 read-out-noise) , with 8 frames acquired for each pattern (four with the positive pattern and four with the negative pattern, to cancel out static aberrations), at 1200Hz, with local turbulence only. The three interaction matrices obtained are shown in Fig. 3, clipped at 1% of their total range in order to visually assess the noise.

Whereas for the "slope-oriented" Hadamard strategy it is possible to distinguish the diagonal zone from the background, some components still do not stand out of the noise in the "voltage-oriented" Hadamard case with this limited calibration time. Compared to the "Zonal" strategy, the noise on the interaction matrices is 52 times lower for the voltage oriented strategy, and 170 times lower for the slope-oriented strategy. These values are not identical to the one in Table

#245856 Received 13 Jul 2015; revised 2 Sep 2015; accepted 2 Sep 2015; published 7 Oct 2015

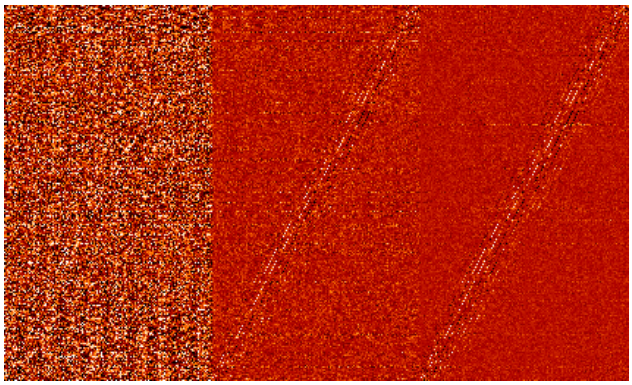

Fig. 3. Experimental SAXO interaction matrices acquired in 90 seconds each, clipped at 1% of the total range. Left: Zonal strategy, Center: Voltage-oriented Hadamard Strategy, Right: Slope-oriented Hadamard strategy. The noise variance in the matrices is estimated to 0.035, 0.00076 and 0.00028 squared pixels.

1, which correspond to the gain in calibration time to reach the same performance. Here, we selected a given experimental calibration time and compare the obtained matrices. The level of noise on the matrices does not convey the final residual phase performance, because it does not take into account the system configuration (the amplitude and shape of the mirror modes for instance) nor the turbulence statistics. However, these experimental results already emphasize the major gain to use slope-oriented Hadamard strategy.

We then stored the interaction matrix acquired with the slope-oriented Hadamard strategy in the system, and tried to close the loop on an artificial source at high flux (1000 photons per subaperture and per frame on the wavefront sensor, 1200Hz, turbulent simulator corresponding to 0.62" seeing and 10m.s^{-1} windspeed [3]). We report that the loop was closed successfully during several minutes, and that we witnessed no performance loss compared to the use of a 1.5 hour acquisition zonal strategy calibration matrix (in both case the estimated Strehl Ratio was worth 92% at 633nm), thus proving that not only the matrix obtained with the slope-oriented Hadamard strategy is less noisy, but also that the matrix is sound, with no missing information or defect that would deteriorate the overall performance.

6. Conclusion

The aim of an interaction matrix calibration process is to obtain the "best" interaction matrix using the minimum amount of time or photons. Intuitively, this can be accomplished by optimizing the signal to noise ratio during calibration: for a given amount of detection noise, one has to maximize the wavefront sensor signal. We have therefore proposed the slope-oriented Hadamard scheme, which consists in using a particular set of independent deformable mirror patterns: they nearly saturate the WFS, producing wave-front measurements close the the bounds of the linearity range. To evaluate our strategy, we have derived a heuristic quality metric corresponding to the miscalibration term of the residual phase variance error budget, and shown how our method tends to optimize this metric. In the case of the SAXO configuration, the gain predicted with our metric was perfectly reproduced with an end-to-end simulation of the SAXO bench, showing a 7 fold gain for the "slope-oriented" Hadamard strategy over the "voltage-oriented" Hadamard strategy, and a 581 gain over the standard "Zonal" strategy, in terms of calibration time. Finally, we have experimentally demonstrated on the SAXO bench

#245856 Received 13 Jul 2015; revised 2 Sep 2015; accepted 2 Sep 2015; published 7 Oct 2015

the feasibility of our method: we have demonstrated that the interaction matrix acquired in 90 seconds with our method was less noisy that with the other techniques, and that it leads to the same closed-loop performance as a reference interaction matrix acquired in 90 minutes with the standard zonal method. Such a gain is of the utmost importance in the context of the future E-ELT, for which maintenance operations will leave a minimal time for interaction matrix calibration. The slope-oriented Hadamard method described in this paper paves the way for an efficient calibration strategy on systems with a high number of degrees of freedom.

A. Residual phase variance due to the miscalibration error

$$\varphi_n^{\text{res},miscal} = M_{\text{DM}} \cdot \left(D^\dagger - \hat{D}^\dagger\right) \cdot M_{\text{WFS}} \cdot \varphi_{n-1}^{\text{res}} \tag{13}$$

We make the assumption that the deformable mirror unseen modes have been filtered out, or conversely that M_{DM} contains no mode unseen by the WFS. Mathematically, this can be expressed as

$$M_{\text{WFS}}^\dagger \cdot M_{\text{WFS}} \cdot M_{\text{DM}} = M_{\text{DM}}. \tag{14}$$

With this, we obtain

$$\begin{aligned}
\varphi_n^{\text{res},miscal} &= M_{\text{DM}} \cdot \left(D^\dagger - \hat{D}^\dagger\right) \cdot M_{\text{WFS}} \cdot \varphi_{n-1}^{\text{res}} \\
&= M_{\text{WFS}}^\dagger \cdot M_{\text{WFS}} \cdot M_{\text{DM}} \cdot \left(D^\dagger - \hat{D}^\dagger\right) \cdot M_{\text{WFS}} \cdot \varphi_{n-1}^{\text{res}} \\
&= M_{\text{WFS}}^\dagger \cdot D \cdot \left(D^\dagger - \hat{D}^\dagger\right) \cdot M_{\text{WFS}} \cdot \varphi_{n-1}^{\text{res}}
\end{aligned} \tag{15}$$

We have $D \cdot \left[D^\dagger - \hat{D}^\dagger\right] = -\Delta D \cdot D^\dagger$ at the first order in ΔD[1] ,which leads to

$$\varphi_n^{\text{res},miscal}(\Delta D) \simeq -M_{\text{WFS}}^\dagger \cdot \Delta D \cdot D^\dagger \cdot M_{\text{WFS}} \cdot \varphi_{n-1}^{\text{res}} \tag{16}$$

With the definition $\mathscr{C}_{\text{slope}} = E\left\{\left(M_{\text{WFS}} \cdot \varphi_{n-1}^{\text{res}}\right)\left(M_{\text{WFS}} \cdot \varphi_{n-1}^{\text{res}}\right)^{\text{T}}\right\}$ and $\|X\|^2_{\mathscr{C}_{\text{slope}}} = \text{Trace}\left[X^{\text{T}}\mathscr{C}_{\text{slope}}X\right]$ and with the identity $X^{\text{T}}\mathscr{C}_{\text{slope}}X = \text{Trace}\left[X\mathscr{C}_{\text{slope}}X^{\text{T}}\right]$, we have

$$\begin{aligned}
\mathscr{E}(\Delta D) &= \text{Var}\ \varphi_n^{\text{res},miscal} \\
&= \text{Trace}\left[E\left\{\left(\varphi_n^{\text{res},miscal}\right)\left(\varphi_n^{\text{res},miscal}\right)^{\text{T}}\right\}\right] \\
&= \text{Trace}\left[M_{\text{WFS}}^\dagger \cdot \Delta D \cdot D^\dagger \cdot E\left\{\left(M_{\text{WFS}} \cdot \varphi_{n-1}^{\text{res}}\right)\left(M_{\text{WFS}} \cdot \varphi_{n-1}^{\text{res}}\right)^{\text{T}}\right\} \cdot \left(M_{\text{WFS}}^\dagger \cdot \Delta D \cdot D^\dagger\right)^{\text{T}}\right] \\
&= \text{Trace}\left[\left(M_{\text{WFS}}^\dagger \cdot \Delta D \cdot D^\dagger\right) \cdot \mathscr{C}_{\text{slope}} \cdot \left(M_{\text{WFS}}^\dagger \cdot \Delta D \cdot D^\dagger\right)^{\text{T}}\right] \\
&= \left\|M_{\text{WFS}}^\dagger \cdot \Delta D \cdot D^\dagger\right\|^2_{\mathscr{C}_{\text{slope}}},
\end{aligned}$$

B. Miscalibration error due to noise during calibration

With Eq. (5) we have $\Delta D \overset{\Delta}{=} D - \hat{D} = -\bar{W} \cdot U^\dagger$, so that $\mathscr{E}(\Delta D) = \left\|M_{\text{WFS}}^\dagger \cdot \bar{W}U^\dagger \cdot D^\dagger\right\|^2_{\mathscr{C}_{\text{slope}}}$. We make the assumption that the calibration noise $\bar{W} = (M_{\text{WFS}} \cdot \phi + W)$ is independent from one actuation pattern to the next and from one wave-front measurement to the next (which is valid

[1] $D \cdot \left[D^\dagger - \hat{D}^\dagger\right] = \left[\hat{D} - D\right] \cdot \hat{D}^\dagger = -\Delta D \cdot \hat{D}^\dagger \simeq -\Delta D \cdot D^\dagger$.

#245856 Received 13 Jul 2015; revised 2 Sep 2015; accepted 2 Sep 2015; published 7 Oct 2015

for the noise part W and for turbulent components ϕ with a high temporal and spatial frequency):

$$\left\langle \bar{W}_{ij}\bar{W}_{k,l}\right\rangle = \delta_{i,k}\delta_{j,l}\sigma_i^2 \tag{17}$$

With this, we gather:

$$\begin{aligned}\left[\left\langle \bar{W}^{\mathrm{T}}\cdot M_{\mathrm{WFS}}^{\dagger,T}\cdot M_{\mathrm{WFS}}^{\dagger}\cdot\bar{W}\right\rangle\right]_{i,j} &= \sum_{k,l}\left\langle \bar{W}_{ik}^{\mathrm{T}}\cdot\left[M_{\mathrm{WFS}}^{\dagger,T}\cdot M_{\mathrm{WFS}}^{\dagger}\right]_{k,l}\cdot\bar{W}_{l,j}\right\rangle \\ &= \sum_{k,l}\left[M_{\mathrm{WFS}}^{\dagger,T}\cdot M_{\mathrm{WFS}}^{\dagger}\right]_{k,l}\left\langle \bar{W}_{ki}\cdot\bar{W}_{l,j}\right\rangle \\ &= \sum_{k,l}\left[M_{\mathrm{WFS}}^{\dagger,T}\cdot M_{\mathrm{WFS}}^{\dagger}\right]_{k,l}\delta_{k,l}\delta_{i,j}\sigma_k^2 \\ &= \left[\sum_{k}\left[M_{\mathrm{WFS}}^{\dagger,T}\cdot M_{\mathrm{WFS}}^{\dagger}\right]_{k,k}\sigma_k^2\right]\cdot\delta_{i,j}\end{aligned} \tag{18}$$

so that $\left\langle \bar{W}^{\mathrm{T}}\cdot M_{\mathrm{WFS}}^{\dagger,T}\cdot M_{\mathrm{WFS}}^{\dagger}\cdot\bar{W}\right\rangle \propto \mathbf{I}\mathrm{d}$. It then follows that:

$$\begin{aligned}\mathscr{E}(\Delta D) &= \left\|M_{\mathrm{WFS}}^{\dagger}\cdot\bar{W}U^{\dagger}\cdot D^{\dagger}\right\|_{\mathscr{C}_{\mathrm{slope}}}^2 \\ &= \mathrm{Trace}\left[\sqrt{\mathscr{C}_{\mathrm{slope}}}^{\mathrm{T}}\cdot\left(D^{\dagger}\right)^{\mathrm{T}}\cdot U^{\dagger,T}\cdot\left\langle \bar{W}^{\mathrm{T}}\cdot M_{\mathrm{WFS}}^{\dagger,T}\cdot M_{\mathrm{WFS}}^{\dagger}\cdot\bar{W}\right\rangle\cdot U^{\dagger}\cdot D^{\dagger}\cdot\sqrt{\mathscr{C}_{\mathrm{slope}}}\right] \\ &\propto \mathrm{Trace}\left[\sqrt{\mathscr{C}_{\mathrm{slope}}}^{\mathrm{T}}\cdot\left(D^{\dagger}\right)^{\mathrm{T}}\cdot U^{\dagger,T}\cdot U^{\dagger}\cdot D^{\dagger}\cdot\sqrt{\mathscr{C}_{\mathrm{slope}}}\right] \\ &= \left\|U^{\dagger}\cdot D^{\dagger}\right\|_{\mathscr{C}_{\mathrm{slope}}}^2\end{aligned} \tag{19}$$

Considering that U and D are full rank matrices, we have $D^{\dagger}D = \mathbf{I}\mathrm{d}$ and $UU^{\dagger} = \mathbf{I}\mathrm{d}$. With the identity $(A^{\dagger}AB)^{\dagger}(ABB^{\dagger})^{\dagger} = (AB)^{\dagger}$, we get $U^{\dagger}D^{\dagger} = (DU)^{\dagger}$, so that:

$$\mathscr{E}(\Delta D) \propto \left\|(DU)^{\dagger}\right\|_{\mathscr{C}_{\mathrm{slope}}}^2 \tag{20}$$

This expression can be further simplified considering the approximation $\mathscr{C}_{\mathrm{slope}} \simeq \mathbf{I}\mathrm{d}$. This is justified for a system where all the low order modes are perfectly compensated, leaving only high order modes showing no correlation from one sub-aperture to the next. For instance, in the case of SAXO, end-to-end simulations (same simulation case as in Fig. 2: 1200Hz 2-frame delay loop, seeing = 0.85" [3]) lead to a nearly diagonal residual slope covariance matrix (non diagonal coefficients are in average 1000 times less energetic than the diagonal coefficients)

We then obtain:

$$\mathscr{E}(\Delta D) \propto \left\|(DU)^{\dagger}\right\|^2 \tag{21}$$

#245856 Received 13 Jul 2015; revised 2 Sep 2015; accepted 2 Sep 2015; published 7 Oct 2015